Optics Communications 285 (2012) 3787–3791

Contents lists available at SciVerse ScienceDirect

Optics Communications

journal homepage: www.elsevier.com/locate/optcom

Spectroscopic investigations on Tb^{3+} doped lead fluoroborate glasses

P. Abdul Azeem [a,*], M. Kalidasan [b], R.R Reddy [c], K Ramagopal [c]

[a] Department of Physics, National Institute of Technology, Kazipet road Hanamakonda, Warangal 506004, A.P., India
[b] Department of Physics, Anna University, Chennai, T.N., India
[c] Department of Physics, Sri Krishnadevaraya University, Anantapur 515003, A.P., India

ARTICLE INFO

Article history:
Received 19 October 2011
Accepted 20 May 2012
Available online 2 June 2012

Keywords:
Glasses
Judd – Ofelt theory
Luminescence
Optical properties
Rare earth

ABSTRACT

This article presents the optical properties of Tb^{3+} in lead fluoroborate glasses of the type X $PbF_2 \cdot (89–X)B_2O_3 \cdot 10\ Al_2O_3 \cdot 1Tb_2O_3$ (where X=8, 12, 16, 20, 24, 28, 34 and 36). The standard Judd–Ofelt model was applied to the room temperature absorption intensities of Tb^{3+} ($4f^8$) to determine the phenomenological intensity parameters Ω_2, Ω_4 and Ω_6. These parameters have been used to calculate radiative transition probabilities (A_{rad}), lifetimes (τ_R) and branching ratios (β_R) for the excited level $^5D_4$. The predicted values of τ_R are compared with the measured values for $^5D_4$ level for eight glass compositions (Glass (A–H)). Among the eight-terbium glasses Glass A with 8 mol% of PbF_2 (as the optimum content) has revealed an intense green emission with maximum life time and higher quantum efficiency. The stimulated emission cross section $\sigma(\lambda_P)$ is also evaluated for the $^5D_4 \rightarrow {}^7F_J$ (J=6, 5, 4 and 3) transitions.

1. Introduction

The study of spectroscopic properties of rare earth doped glasses has gained importance, since a complete knowledge on the fundamental data that includes optical efficiency, transition positions, transition probabilities, radiative and non-radiative decay rates, branching ratios etc. for the excited states is essential to estimate/design optical devices such as lasers, color displays, upconverters, optical fibers and optical amplifiers and so on [1–5]. Rare earth ion doped glasses have obtained considerable interest due to their more homogeneous luminescence, low cost, greater ease of production and possibility of adjusting composition in comparison with other luminescent materials [6]. Among the trivalent rare-earth ions, the Tb^{3+} has considerable interest due to its stimulated green emission through the $^5D_4 \rightarrow {}^7F_5$ (543 nm) transition. The large energy difference (14,663 cm^{-1}) between the $^7F_{J=0-6}$ multiplet levels and $^5D_4$ emitting level, the luminescence property of Tb^{3+} has been proven to be useful in characterizing the energy level structure and optical transition mechanism. The absorption and luminescence spectra of Tb^{3+} ion in different lattices have been studied by several workers [7–9].

In this paper an attempt has made to analyze the optical properties of Tb^{3+} doped lead fluoroborate glasses of the type X $PbF_2 \cdot (89–X)B_2O_3 \cdot 10Al_2O_3 \cdot 1Tb_2O_3$ (where X=8, 12, 16, 20, 24, 28, 32, 36). The Judd–Ofelt theory [10,11] has been applied to interpret the local environment of Tb^{3+} ions and bond covalency of RE–O bond. Using Judd–Ofelt [10,11] theory, radiative transition probabilities (A_{rad}), radiative lifetimes (τ_R) and branching ratios (β_R) have been computed for the excited level $^5D_4$ of Tb^{3+} in these lead fluoroborate glasses. Emission spectra of these rare earth glasses are also studied. Luminescence decay curves of the $^5D_4$ level of Tb^{3+} ions in lead fluoroborate glasses have been measured and analyzed.

2. Experimental studies

The Tb^{3+} doped lead fluoroborate glasses were prepared by using appropriate amounts of analar-quantity B_2O_3, PbF_2, Al_2O_3 and Tb_2O_3 with 99.99% purity. For convenience these glass systems are designated as A, B, C, D, E, F, G and H according to the PbF_2 content in the glass matrix:

GLASS A: 8 $PbF_2 \cdot 81\ B_2O_3 \cdot 10\ Al_2O_3 \cdot 1\ Tb_2O_3$
GLASS B: 12 $PbF_2 \cdot 77\ B_2O_3 \cdot 10\ Al_2O_3 \cdot 1\ Tb_2O_3$
GLASS C: 16 $PbF_2 \cdot 73\ B_2O_3 \cdot 10\ Al_2O_3 \cdot 1\ Tb_2O_3$
GLASS D: 20 $PbF_2 \cdot 69\ B_2O_3 \cdot 10\ Al_2O_3 \cdot 1\ Tb_2O_3$
GLASS E: 24 $PbF_2 \cdot 65\ B_2O_3 \cdot 10\ Al_2O_3 \cdot 1\ Tb_2O_3$
GLASS F: 28 $PbF_2 \cdot 61\ B_2O_3 \cdot 10\ Al_2O_3 \cdot 1\ Tb_2O_3$
GLASS G: 32 $PbF_2 \cdot 57\ B_2O_3 \cdot 10\ Al_2O_3 \cdot 1Tb_2O_3$
GLASS H: 36 $PbF_2 \cdot 53\ B_2O_3 \cdot 10\ Al_2O_3 \cdot 1Tb_2O_3$

The samples are prepared by conventional melt quenching technique [12–14]. All the chemicals used for the present work

* Corresponding author.
E-mail address: drazeem2002@gmail.com (P. Abdul Azeem).

0030-4018/$ - see front matter © 2012 Elsevier B.V. All rights reserved.
http://dx.doi.org/10.1016/j.optcom.2012.05.034

were procured from the Sigma–Aldrich. About 5 gm batches of the compositions were weighed accurately using an electronic microbalance and thoroughly grinded in an agate mortar to homogenize the constituents. The batches taken in a platinum crucible were then melted in an electrical furnace in the range of 1150 °C to 1200 °C for 1 h. The melt was poured onto a preheated brass mold and annealed at 350 °C (above which the sample may lose its glassy nature) for about 5 h to remove thermal strains. Then the glass samples were allowed to cool to room temperature (RT) and were well polished for optical measurements. The refractive indices, n_d were measured using an Abbe refractometer at sodium wavelength (589.3 nm) with 1-Bromonaphthalin ($C_{10}H_7Br$) as contact liquid. The density of the glass samples were determined by the Archimede's method, using xylene as an immersion liquid. Absorption spectra were recorded at room temperature (RT) on a spectrophotometer (Varian Carry 5E model) in the wavelength range of 300–2500 nm with spectral resolution of 1 nm. The excitation and emission spectra for the glass samples under study were recorded in HORIBA JOBIN YVON SPEX Fluorolog-3–11 Spectrofluorometer. The decay profile of the glass samples under study was recorded using HORIBA JOBIN YVON SPEX Fluorolog-3 Model FL3–22 Fluorimeter. The measurement was carried out for the prominent fluorescent line $^5D_4 \rightarrow {}^7F_5$(543 nm) with 369 nm UV excitation for all eight glass system. The experimental lifetime of the fluorescent level of Ln ions was determined by first e-folding time of the decay profile [8,15]. The system employs the DFS software in acquiring the spectra and decay curves. The total life time can be determined experimentally by measuring the luminescence decay for the respective transitions.

3. Results and discussion

3.1. Absorption spectra

Fig. 1 illustrates the room temperature absorption spectra of Terbium doped lead fluoroborate glasses in the spectral region 300–2500 nm. A total of six absorption bands: $^7F_6 \rightarrow {}^5L_9, {}^5L_{10}, {}^5G_6, {}^5D_4, {}^7F_2, {}^7F_3$ are observed. The spectral intensities for the observed bands in the absorption spectra of these glasses, which are often expressed in terms of oscillator strength of forced electronic dipole transitions, have been analyzed with the help of Judd–Ofelt (J–O) theory [10,11] using the expressions available in literature and the values are tabulated in Table 1. The comparison of experimental and theoretical oscillator strengths shows a reasonable agreement. The rms deviations of oscillator strengths of experimental and calculated values are given in Table 1. The relatively small values of these deviations confirm the validity and applicability of J–O theory for the present glass system.

The J–O Intensity parameters (Ω_λ) have been calculated from the absorption bands by using the least-square fitting analysis of the experimental oscillator strengths using matrix elements [16] and are presented in Table 1. The J–O intensity parameters (Ω_λ) are phenomenological characteristics for the influence of surrounding environment of the rare earth ions as they contain implicitly the crystal field terms and the radial integral wave functions. These parameters play an important role to investigate the coordination environment as well as bonding in the vicinity of rare-earth ions. The obtained values of the intensity parameters (Ω_λ, $\lambda=2, 4, 6$) are presented in Table 1. On overall consideration, in eight glass hosts the trend is as follows,

$$\Omega_2 > \Omega_6 > \Omega_4.$$

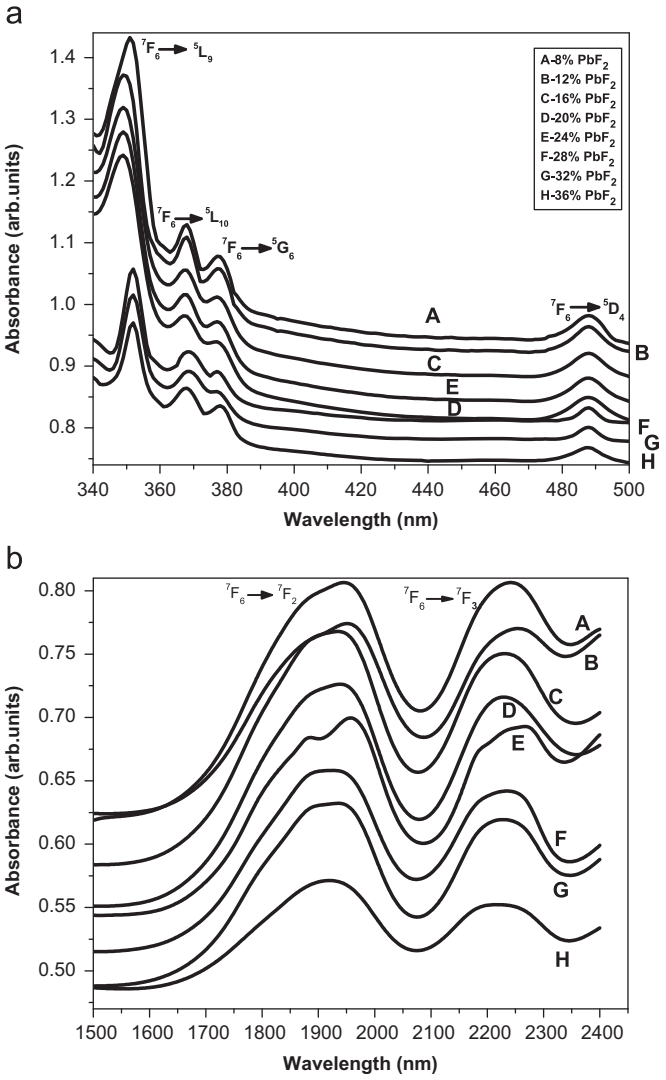

Fig. 1. (a) Room temperature optical absorption spectra of Tb^{3+} doped lead fluoroborate glasses at lower wavelength region. (b) Room temperature optical absorption spectra of Tb^{3+} doped lead fluoroborate glasses at higher wavelength region (1500–2500 nm).

In general, the parameter Ω_2 is related to the covalency and/or structural changes in the vicinity of the Tb^{3+} ion (short range effect) and Ω_4 related to the long range effects. From Table 1 it is observed that the Ω_2 value for Glass A is found to be greater than other glasses, this observation points out that the lead ions occupy the network-forming positions and result a strong field around Tb^{3+} ion and minimize the Tb–O average distance. Larger value of Ω_2 for Glass A indicates that stronger covalency of the Tb–O bonds and lower symmetry for the Tb^{3+} ions than other glass systems. It is also observed that Ω_2 is decreasing with increasing in PbF_2 content this decrease of the covalent nature of the bonds around Tb is certainly due to an increase of the ionic character and due to the presence of fluorine ions surrounding Tb. However, the magnitude of Ω_4 and Ω_6 parameters has been related to the rigidity of the medium in which the ions are situated.

3.2. Excitation and emission spectra

The excitation spectrum was recorded in the wavelength region 300 nm to 400 nm for 543 nm emission of Tb^{3+} (with xenon excitation) is shown in Fig. 2, which is due to the 4f–4f

Table 1
Experimental (f_{exp}), calculated (f_{cal}) oscillator strengths ($\times 10^6$) and Judd–Ofelt intensity ($\Omega_\lambda \times 10^{20}$ cm^2) parameters of prepared Tb^{3+} doped lead fluoroborate glasses.

Energy level	Glass A		Glass B		Glass C		Glass D		Glass E		Glass F		Glass G		Glass H	
	f_{exp}	f_{cal}	f_{exp}	f_{cal}	f_{exp}	f_{cal}	f_{exp}	f_{cal}	f_{exp}	f_{cal}	f_{exp}	f_{cal}	f_{exp}	f_{cal}	f_{exp}	f_{cal}
$^7F_6 \rightarrow {}^5L_9$	0.719	0.720	0.654	0.656	0.593	0.619	0.500	0.561	0.587	0.603	0.581	0.580	0.566	0.567	0.544	0.543
$^7F_6 \rightarrow {}^5L_{10}$	0.850	0.853	0.770	0.775	0.704	0.729	0.683	0.665	0.710	0.714	0.603	0.685	0.630	0.672	0.609	0.641
$^7F_6 \rightarrow {}^5G_6$	0.251	0.247	0.202	0.232	0.201	0.222	0.219	0.204	0.224	0.220	0.212	0.209	0.194	0.205	0.182	0.200
$^7F_6 \rightarrow {}^5D_4$	0.040	0.041	0.032	0.039	0.030	0.038	0.029	0.036	0.030	0.039	0.033	0.036	0.041	0.035	0.032	0.034
$^7F_6 \rightarrow {}^7F_2$	1.301	1.320	1.198	1.209	1.144	1.138	1.016	1.037	1.137	1.116	1.065	1.070	1.062	1.050	1.116	1.008
$^7F_6 \rightarrow {}^7F_3$	1.240	1.257	1.160	1.167	1.000	1.106	1.103	1.000	1.076	1.090	1.037	1.039	0.967	1.020	0.977	1.002
σ	0.011		0.014		0.046		0.051		0.013		0.034		0.029		0.048	
Ω_2	9.051		8.780		8.619		8.198		8.541		7.921		7.586		7.469	
Ω_4	2.518		2.388		2.270		1.954		2.203		2.026		2.012		2.153	
Ω_6	4.569		4.015		3.712		3.307		3.498		3.315		3.271		3.137	

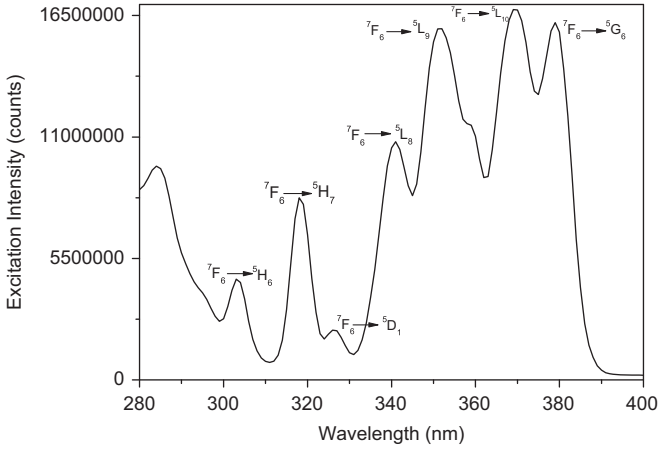

Fig. 2. UV Excitation spectra of Tb^{3+} doped lead fluoroborate glasses.

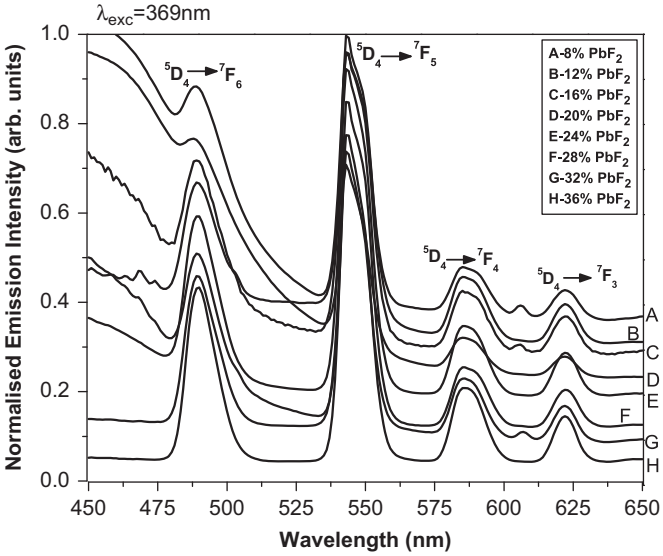

Fig. 3. Emission spectra of Tb^{3+} doped lead fluoroborate glasses excited at 369 nm.

transitions. The transitions assigned to those bands are $^7F_6 \rightarrow {}^5H_6, {}^5H_7, {}^5D_1, {}^5L_8, {}^5L_9, {}^5G_5, {}^5L_{10}, {}^5G_6$. The excitation spectrum shows an agreement with absorption spectra.

Among different excitation transitions, $^7F_6 \rightarrow {}^5L_{10}$ (369 nm) is more prominent. This has been used to measure emission spectra of Tb^{3+} doped lead fluoroborate glasses as shown in Fig. 3. The emission transitions have shown sharp emission bands due

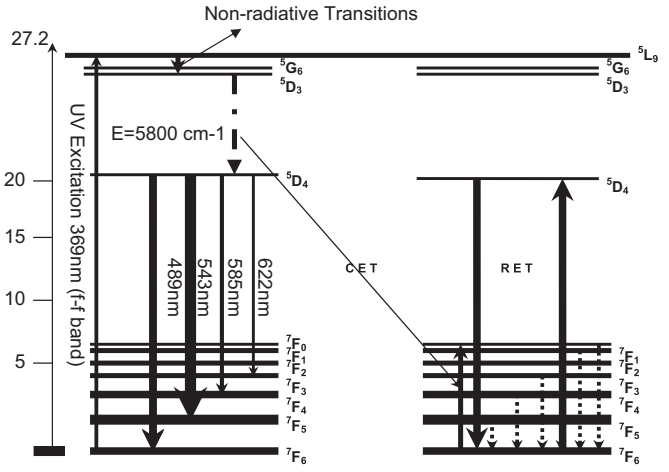

Fig. 4. A schematic energy level diagram of the luminescence and the resonant energy transfer processes in Tb^{3+} doped lead fluoroborate glasses.

to the f–f inner shell transitions, from the excited level to the lower level such as $^5D_4 \rightarrow {}^7F_J$ (J=3 to 6) for Tb^{3+}. From emission spectra, transitions such as $^5D_4 \rightarrow {}^7F_6$ (489 nm), $^5D_4 \rightarrow {}^7F_5$ (543 nm), $^5D_4 \rightarrow {}^7F_4$ (585 nm) and $^5D_4 \rightarrow {}^7F_3$ (622 nm) have been identified [17,18]. The assignments of the transitions are taken from Dieke and Crosswhite [19] and are expressed formally in the LS coupling. Of them, 543 nm has shown bright green emission, arising from the Laporte-forbidden $^5D_4 \rightarrow {}^7F_5$ transition [20]. The transition $^5D_4 \rightarrow {}^7F_6$ obeys the magnetic dipole (MD) transition selection rule of $\Delta J = \pm 1$ [17,21].

When Tb^{3+} ions excited by UV radiation, electronic transition of either $^5D_3 \rightarrow {}^7F_J$ (blue emission) or successive $^5D_3 \rightarrow {}^5D_4$ and $^5D_4 \rightarrow {}^7F_J$ (green emission) takes place, where J=3, 4, 5 and 6. The energy level diagram of the luminescence and the resonant energy transfer processes in Tb^{3+} doped lead fluoroborate glasses is as shown in Fig. 4. The small energy gap between (5800 cm^{-1}) between the $^5D_4$ and $^5D_3$ emission levels causes a fast non-radiative decay and enhances the population of $^5D_4$ level much more at higher Tb^{3+} concentrations resulting the enhancement of luminescence intensity. Luminescence from the higher excited state such as $^5D_3$ was not detected, indicating a very efficient non-radiative relaxation to the lowest excited $^5D_4$ levels. As shown in Fig. 3, it was noted that the blue emission from $^5D_3$ level to ^7F_J multiplets is absent in all eight glasses. The observation can be rationalized by the fact that the emission derived from $^5D_3$ level may be quenched by two types of nonradiative relaxation process, viz., cross-relaxation mechanism and multiphonon mechanism that result in the rapid population of the $^5D_4$ level at the expense of $^5D_3$ [22,23].

Table 2
Emission band position (λ_P nm), effective bandwidths ($\Delta\lambda_{eff}$ nm), stimulated emission cross-section ($\sigma(\lambda_P) \times 10^{22}$ cm^2) for the measured fluorescent transitions of prepared Tb^{3+} doped lead fluoroborate glasses.

Transition	parameter	A	B	C	D	E	F	G	H
$^5D_4 \rightarrow {}^7F_6$	λ_P	490	489	488	489	489	489	489	489
	$\Delta\lambda_{eff}\ \sigma$	13.265	12.858	15.135	13.323	14.877	13.989	14.009	14.314
	(λ_P)	0.928	0.927	0.767	0.824	0.790	0.794	0.765	0.735
$^5D_4 \rightarrow {}^7F_5$	λ_P	543	543	543	543	543	543	543	543
	$\Delta\lambda_{eff}\sigma$	11.884	11.204	10.186	12.063	12.402	12.149	12.264	11.875
	(λ_P)	9.939	10.532	11.514	9.411	9.698	9.310	8.800	8.900
$^5D_4 \rightarrow {}^7F_4$	λ_P	585	586	585	586	585	585	585	585
	$\Delta\lambda_{eff}\ \sigma$	13.988	13.014	13.085	14.194	14.284	14.695	13.721	14.054
	(λ_P)	0.905	0.932	0.890	0.750	0.816	0.749	0.784	0.767
$^5D_4 \rightarrow {}^7F_3$	λ_P	622	622	622	622	622	622	622	622
	$\Delta\lambda_{eff}\sigma$	9.627	9.865	9.890	10.583	10.704	11.320	10.557	10.478
	(λ_P)	2.455	2.384	2.358	2.124	2.230	1.983	2.033	2.009

The following cross relaxation may also occur:

$$Tb^{3+}\ (^5D_3) + Tb^{3+}\ (^7F_6) \rightarrow Tb^{3+}\ (^5D_4) + Tb^{3+}\ (^7F_0)$$

So that the $^5D_3$ to ^7F_J transitions of some high Tb^{3+} (≥ 1.0 mol%) concentration materials are quenched by the energy transfer process as mentioned above. Thus only $^5D_4$ to ^7F_J emission can be observed.

Table 2 gives the peak wavelengths (λ_P), effective band widths ($\Delta\lambda_{\text{eff}}$), and the stimulated emission cross-sections σ (λ_P), for the four transitions $^5D_4 \rightarrow {}^7F_6, {}^7F_5, {}^7F_4, {}^7F_3$. The stimulated emission cross-section for the $^5D_4 \rightarrow {}^7F_5$ transition is the highest for all the eight glass systems, which indicates that the laser efficiency for this transition is high.

3.3. Radiative properties

The J–O intensity parameters (Ω_λ) have been used to compute the radiative properties of emission characteristics of the Tb^{3+} doped lead fluoroborate glasses. Using the standard formulae available in literature [24–26] the radiative properties have been calculated for the $^5D_4 \rightarrow {}^7F_J$ (J=3, 4, 5 and 6) transitions for the eight glass systems and these values are presented in Table 3. The radiative properties of Tb^{3+} ions (or any of the Ln^{3+}ions) depend on the number of factors such as property of network former and modifier of glass. The parameter β_R (i.e., the branching ratio) of the luminescent transitions characterizes the lasing power of the potential laser transitions. The β_R values obtained for the luminescent transitions originated from $^5D_4$ for all the eight glasses are furnished in Table 3. It is well established that an emission transition having branching ratio ≥ 0.50 can emit laser radiation more efficiently [27]. Among various transitions the transition $^5D_4 \rightarrow {}^7F_5$ is found to have the highest values of β_R for all the eight glasses which is the characteristic property of Tb^{3+} ion. This transition may therefore be considered as a possible laser transition. Higher the emission probability for a transition leads to faster decay of that level and hence shortening of the lifetime. It was seen from Table 3 that the spontaneous emission probability (A) and the total emission probability (A_T) is smaller for Glass A and hence it is having higher excited state lifetimes compare to the other glass systems. The lifetimes (τ_R) of $^5D_4 \rightarrow {}^7F_5$ of all the eight glasses shows a decreasing trend with increasing PbF_2 content. The lower is the modifying action of the NWM in the glass network (Higher is the rigidity of the network), lower is the radiative lifetime and the greater presence of higher vibrational frequencies [28]. Such vibrations lead to non-radiative losses in the glass systems with increasing PbF_2. Even we have observed decrease in the intensity with increase PbF_2 content. The small difference in experimental and calculated lifetimes can be attributed to non-radiative decay.

From Table 3 it is observed that the Glass A (8% PbF_2) having higher values in both experimental and calculated lifetimes for $^5D_4 \rightarrow {}^7F_5$ transition is then the best glass to exhibit better lasing action among the eight glasses with a higher quantum efficiency of 95.63%.

3.4. Decay analysis

Analysis of decay curves gives information about the measured life times of the excited states of trivalent RE ions in any host composition. For a detailed study of the quenching of the fluorescence, we have measured the decay profile for the $^5D_4 \rightarrow {}^7F_5$ (green fluorescence) transition at 543 nm of Tb^{3+} in lead fluoroborate glasses excited with 369 nm. The plots of the intensity of the $^5D_4 \rightarrow {}^7F_5$ transition for different concentrations of PbF_2 are shown in Fig. 5. At lower Tb^{3+} concentrations (≤ 0.5 mol%), the decay curves exhibited single-exponential nature and at higher concentrations (≥ 1.0 mol%) they exhibited non-exponential behavior due to the resonance energy transfer among the excited Tb^{3+} ions through $(^5D_4, {}^7F_6) \rightarrow ({}^7F_6, {}^5D_4)$ transitions as show in Fig. 4.

These curves were subjected to appropriate mathematical fitting procedures in order to determine the first e-folding times of the decay curves of the excited state using origin software and the values are presented in Table 3, which shows that the Glass A is having higher fluorescence life time. The decay time was found to be decreasing as we go down the order from Glass A to Glass H indicates a rapid energy transfer or resonant energy transfer (RET) among the excited Tb^{3+} ions with increasing PbF_2 content. In such a case, the Tb^{3+} ions may play an intermediate role in the recombination reaction either through bypassing or by resonant energy transfer condition, leading to a decrease in the radiative transitions [29].

4. Conclusions

The calculated intensity parameters follows the trend $\Omega_2 > \Omega_6 > \Omega_4$ in all the glass systems. The value of Ω_2 is found to be higher for Glass A, it shows that the covalency is stronger between the Tb^{3+} and Oxygen ion of the glass matrix compared to other glasses. The emission spectra of all the eight glass systems show that the Glass A with 8% PbF_2 is having the higher intensity for the prominent green emission. The transition $^5D_4 \rightarrow {}^7F_5$ is found to have the highest values of β_R for all the eight glasses and therefore this transition is the potential laser transition. It is also observed that the stimulated emission

Table 3
Radiative properties (A,A_T, β_R,τ_R) and Quantum efficiency (η %) of the fluorescent levels of prepared Tb^{3+} doped lead fluoroborate glasses.

Glass	Transition	Energy ν (cm^{-1})	A (s^{-1})	β_R
A	$^5D_4\rightarrow{}^7F_6$	20,408	38.468	0.116
	$^5D_4\rightarrow{}^7F_5$	18,416	244.845	0.739
	$^5D_4\rightarrow{}^7F_4$	17,094	19.477	0.059
	$^5D_4\rightarrow{}^7F_3$	16,077	28.449	0.086
			A_T (s^{-1})=331.240	
			$\tau_{R(cal)}$ (ms)=3.019	$\tau_{R(exp)}$ (ms)=2.887
			η %=95.63	
B	$^5D_4\rightarrow{}^7F_6$	20,450	39.944	0.114
	$^5D_4\rightarrow{}^7F_5$	18,416	260.029	0.743
	$^5D_4\rightarrow{}^7F_4$	17,065	19.708	0.056
	$^5D_4\rightarrow{}^7F_3$	16,077	30.103	0.086
			A_T (s^{-1})=349.785	
			$\tau_{R(cal)}$ (ms)=2.859	$\tau_{R(exp)}$ (ms)=2.637
			η %=92.24	
C	$^5D_4\rightarrow{}^7F_6$	20,492	40.304	0.113
	$^5D_4\rightarrow{}^7F_5$	18,416	265.636	0.746
	$^5D_4\rightarrow{}^7F_4$	17,094	19.587	0.055
	$^5D_4\rightarrow{}^7F_3$	16,077	30.673	0.086
			A_T (s^{-1})=356.200	
			$\tau_{R(cal)}$ (ms)=2.807	$\tau_{R(exp)}$ (ms)=2.517
			η %=89.67	
D	$^5D_4\rightarrow{}^7F_6$	20,450	39.204	0.110
	$^5D_4\rightarrow{}^7F_5$	18,416	266.745	0.751
	$^5D_4\rightarrow{}^7F_4$	17,065	18.451	0.052
	$^5D_4\rightarrow{}^7F_3$	16,077	30.6692	0.086
			A_T (s^{-1})=355.069	
			$\tau_{R(cal)}$ (ms)=2.816	$\tau_{R(exp)}$ (ms)=2.382
			η %=84.59	
E	$^5D_4\rightarrow{}^7F_6$	20,450	42.927	0.111
	$^5D_4\rightarrow{}^7F_5$	18,416	288.833	0.749
	$^5D_4\rightarrow{}^7F_4$	17,094	20.776	0.054
	$^5D_4\rightarrow{}^7F_3$	16,077	33.287	0.086
			A_T (s^{-1})=385.822	
			$\tau_{R(cal)}$ (ms)=2.592	$\tau_{R(exp)}$ (ms)=2.288
			η %=88.27	
F	$^5D_4\rightarrow{}^7F_6$	20,450	41.337	0.112
	$^5D_4\rightarrow{}^7F_5$	18,416	276.86	0.748
	$^5D_4\rightarrow{}^7F_4$	17,094	20.002	0.054
	$^5D_4\rightarrow{}^7F_3$	16,077	31.92	0.086
			A_T (s^{-1})=370.124	
			$\tau_{R(cal)}$ (ms)=2.702	$\tau_{R(exp)}$ (ms)=2.237
			η %=82.79	
G	$^5D_4\rightarrow{}^7F_6$	20,450	39.499	0.113
	$^5D_4\rightarrow{}^7F_5$	18,416	261.677	0.746
	$^5D_4\rightarrow{}^7F_4$	17,094	19.352	0.055
	$^5D_4\rightarrow{}^7F_3$	16,077	30.222	0.086
			A_T (s^{-1})=350.751	
			$\tau_{R(cal)}$ (ms)=2.851	$\tau_{R(exp)}$ (ms)=2.263
			η %=79.38	
H	$^5D_4\rightarrow{}^7F_6$	20,450	38.435	0.113
	$^5D_4\rightarrow{}^7F_5$	18,416	254.109	0.745
	$^5D_4\rightarrow{}^7F_4$	17,094	19.233	0.056
	$^5D_4\rightarrow{}^7F_3$	16,077	29.393	0.086
			A_T (s^{-1})=341.170	
			$\tau_{R(cal)}$ (ms)=2.931	$\tau_{R(exp)}$ (ms)=2.245
			η %=76.60	

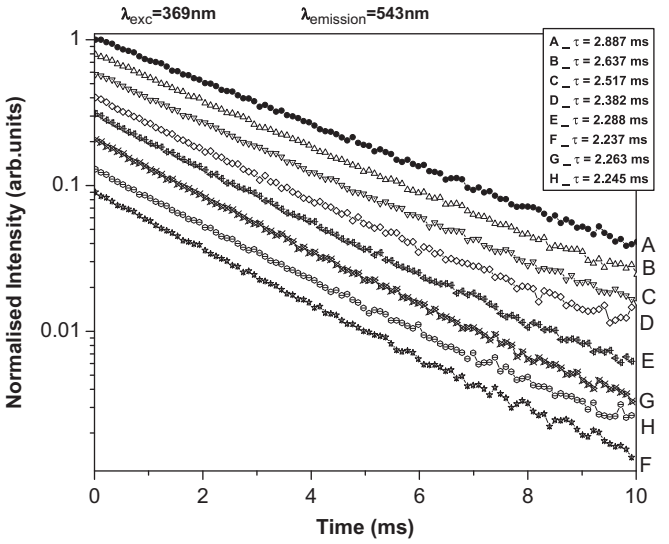

Fig. 5. Logarithmic plot of the decay curves of the Tb3+ doped lead fluoroborate glasses for $^5D_4\rightarrow{}^7F_5$ (543 nm) transition excited at 369 nm.

crosssection for the $^5D_4\rightarrow{}^7F_5$ transition is the highest for all the eight glass systems, which indicates that the laser efficiency for this transition is high. In conclusion, this study shows that Tb^{3+} doped lead fluoroborate glasses possesses several competitive spectroscopic properties, suggesting that Glass A with 8% PbF_2 has potential candidate for 0.54 μm laser operation.

References

[1] B. Padlyak, W. Ryba-Romanowski, R. Lisieck, V. Adamiv, Y. Buraki, I. Teslyuk, A. Banaszak-Piechowska, Optique AppliquTe 2 (2010) 427.
[2] A. Mohan Babu, B.C. Jamalaiah, T. Suhasini, T. Srinivasa Rao, L. Rama Moorthy, Solid State Sciences 13 (2011) 574.
[3] J.H. Choi, F.G. Shi, A. Margaryan, A. Margaryan, W. van der Veer, Journal of Alloys and Compounds 450 (2008) 540.
[4] M. Yamaga, B. Henderson, K.P. O'Donnell, Y. Gao, Physsical Review B 44 (1991) 4853.
[5] V.D. Rodríuez, V.K. Tikhomirov, J. Médez-Ramos, A.C. Yanes, V.V. Moshchalkov, Solar Energy Materials and Solar Cells 94 (2010) 1612–1617.
[6] K. Tonooka, N. Kamata, K. Yamada, F. Maruyama, Journal of Non-Crystalline Solids 150 (1992) 185.
[7] A. Agnesi, P. Dallocchio, F. Pirzio, G. Reali, Optics Communication 282 (2009) 2070.
[8] B.C. Jamalaiah, M.V. VijayaKumar, K. RamaGopal, Physica B 406 (2011) 2871–2875.
[9] V.K. Rai, S.B. Rai, D.K. Rai, J. Mater. Sci. 39 (2004) 4971.
[10] B.R. Judd, Physsical Review 127 (1962) 750–761.
[11] G.S. Ofelt, J. Chem. Phys. 37 (1962) 511–520.
[12] A. Paul, Chemistry of glasses, Chapman & Hall, London, 1982.
[13] S.R. Eliot, Physics of Amorphous Materials, Longman, London, 1990.
[14] J.F. Shackl Ford, Introduction to Materials Science for Engineers, Macmillan, New York, 1985.
[15] C.K. Jayasankar, P. Babu, Th.TroK ster and W.B. Holzapfel, Journal of Luminescence 91 (2000) 33.
[16] W.T. Carnall, P.R. Fields, K. Rajnak, J.Chem. Phys. 49 (1968) 4424.
[17] G. Lakshminarayana, J. Qiu, J.Alloys compd. 476 (2009) 720.
[18] C.H. Kam, S. Buddhudu, Physica B 344 (2004) 182.
[19] G.H. Dieke, Spectra and Energy Levels of Rare Earth Ions in Crystals, in: H.M. Crosswhite, H. Crosswhite (Eds.), Interscience Publishers, New York, 1968.
[20] Z. Xu, Y. Li, Z. Liu, D. Way, Journal of Alloys and Compounds 391 (2005) 202.
[21] N. Duhamel-Henry, J.L. Adam, B. Jacquier, C. Linares, Optical Materials 5 (1996) 197.
[22] Y.S. Chang, H.J. Liu, Y.C. Li, Y.L. Chai, Y.Y. Tsai, Journal of Solid State Chemistry 180 (2007) 3076.
[23] F.S. Kao, Teng-Ming Chen, Journal of Luminescence 96 (2002) 261–267.
[24] S. Balaji, P. Abdul Azeem, R.R. Reddy, Physica B 394 (2007) 62–68.
[25] C. Gorller-Walrand, K. Binnemans, Spectral intensities of f–f transition, in: K.A. Gschneidner Jr., L. Eyring (Eds.), Handbook on the Physics and Chemistry of Rare Earths, 25, North-Holland, Amsterdam, 1998, Chapter 167.
[26] M.B. Saisudha, J. Ramakrishna, Physsical Review B 53 (1995) 10.
[27] J.L. Adam, W.A. Sibley, Journal of Non-Crystalline Solids 16 (1985) 267.
[28] S.V.G.V.A. Prasad, M. Srinivasa Reddy, V..Ravi Kumar, N..Veeraiah, 127(2007)637.
[29] P. Nageswara Rao, D. Krishna Rao, N. Veeraiah, Journal of Luminescence 117 (2006) 53.